Published in final edited form as:
Exp Neurol. 2012 July ; 236(1): 122–130. doi:10.1016/j.expneurol.2012.04.007.

Novel aspirin-triggered Neuroprotectin D1 attenuates cerebral ischemic injury after experimental stroke

Nicolas G. Bazan[a,*], **Tiffany N. Eady**[a], **Larissa Khoutorova**[a], **Kristal D. Atkins**[a], **Song Hong**[a], **Yan Lu**[a], **Changde Zhang**[a], **Bokkyoo Jun**[a], **Andre Obenaus**[b], **Gabrielle Fredman**[c], **Min Zhu**[d], **Jeremy W. Winkler**[d], **Nicos A. Petasis**[d], **Charles N. Serhan**[c], and **Ludmila Belayev**[a]

[a]Neuroscience Center of Excellence, School of Medicine, Louisiana State University Health Sciences Center, New Orleans, LA 70112, USA

[b]Non-Invasive Imaging Laboratory, Departments of Radiation Medicine, Radiology, Pediatrics, Biophysics and Bioengineering, Loma Linda University, Loma Linda, CA 92354 USA

[c]Center for Experimental Therapeutics and Reperfusion Injury, Harvard Institutes of Medicine, Department of Anesthesiology, Perioperative, and Pain Medicine, Brigham and Women's Hospital, and Harvard Medical School, Boston, MA, 02115, USA

[d]Department of Chemistry and Loker Hydrocarbon Research Institute, University of Southern California, Los Angeles, CA 90089, USA

Abstract

Acute ischemic stroke triggers complex neurovascular, neuroinflammatory and synaptic alterations. Aspirin and docosahexaenoic acid (DHA), an omega-3 essential fatty acid family member, have beneficial effects on cerebrovascular diseases. DHA is the precursor of neuroprotectin D1 (NPD1), which downregulates apoptosis and, in turn, promotes cell survival. Here we have tested the effect of aspirin plus DHA administration and discovered the synthesis of aspirin-triggered NPD1 (AT-NPD1) in the brain. Then we performed the total chemical synthesis of this molecule and tested in the setting of 2h middle cerebral artery occlusion (MCAo) in Sprague-Dawley rats. Neurological status was evaluated at 24h, 48h, 72h, and 7 days. At 3h post-stroke onset, an intravenous administration of 333μg/kg of AT-NPD1 sodium salt (AT-NPD1-SS) or methyl-ester (AT-NPD1-ME) or vehicle (saline) as treatment was given. On day 7, *ex vivo* magnetic resonance imaging (MRI) of the brains was conducted on 11.7T MRI. T2WI, 3D volumes, and apparent diffusion coefficient (ADC) maps were generated. In addition, infarct volumes and number of GFAP (reactive astrocytes), ED-1 (activated microglia/macrophages) and SMI-71-positive vessels were counted in the cortex and striatum at the level of the central lesion. All animals showed similar values for rectal and cranial temperatures, arterial blood gases, and plasma glucose during and after MCAo. Treatment with both AT-NPD1-SS and AT-NPD1-ME significantly improved neurological scores compared to saline treatment at 24h, 48h, 72h and 7 days. Total lesion volumes computed from T2WI images were significantly reduced by both AT-NPD1-SS and AT-NPD1-ME treatment in the cortex (by 44% and 81%), striatum (by 61% and 77%) and total infarct (by 48% and 78%, respectively). Brain edema, computed from T2WI in the cortex (penumbra) and striatum (core), was elevated in the saline group. In contrast, both AT-

Correspondence to: Nicolas G. Bazan, 2020 Gravier Street, Suite D, Neuroscience Center of Excellence, Louisiana State University Health Sciences Center, New Orleans, LA 70112. Phone: 504-599-0831; Fax: 504-568-5801; nbazan@lsuhsc.edu.

NPD1 decreased water content in the striatum on day 7. 3D volumes, computed from T2WI, were dramatically reduced with both AT-NPD1 and the lesion was mostly localized in the subcortical areas. Treatment with both AT-NPD1-SS and AT-NPD1-ME significantly reduced cortical (by 76% and 96%), subcortical (by 61% and 70%) and total (69% and 84%, respectively) infarct volumes as defined by histopathology. In conclusion, a novel biosynthetic pathway that leads to the formation of AT-NPD1 mediator in the brain was discovered. In addition, administration of synthetic AT-NPD1, in either its sodium salt or as the methyl ester, was able to attenuate cerebral ischemic injury which leads to a novel approach for pharmaceutical intervention and clinical translation.

Keywords

Neuroprotectin D1; Docosahexaenoic acid; Aspirin; Stroke; Middle cerebral artery occlusion; Cerebral ischemia; Behavior; Histopathology; Rat

Introduction

Stroke is a major cause of death and disability worldwide (Donnan et al., 2008) and remains a challenging condition without effective therapy (Iadecola and Anrather, 2011; Moskowitz et al., 2010; Ratan, 2010). Tissue plasminogen activator is the only therapeutic option available for stroke treatment, but its use is restricted by a narrow therapeutic window and only 3-5% of patients qualify for this therapy. Acute ischemic stroke lesions encompass the penumbra, an area of hypoperfusion surrounding the core with a limited lifespan of a few hours unless reperfusion is initiated. Despite this short window, the penumbra is potentially salvageable and is a target for neuroprotection (Lo, 2008).

Antithrombotic therapy, mainly with aspirin, reduces vascular events (myocardial infarction, ischemic stroke) in subjects with increased risk of ischemic stroke (Yip and Benavente, 2011). Unlike current anti-inflammatory agents, which delay resolution and can be harmful (Schwab et al, 2007), aspirin accelerates resolution mainly due to cyclooxygenase (COX)-1 acetylation at its catalytic site, thus blocking formation of endoperoxide prostaglandin G2 and biosynthesis of thromboxanes and prostaglandins.

Omega-3 essential fatty acids (found in fish oils) are of increasing interest for managing cerebrovascular disease (Bazan, 2007; Kakar et al., 2008). Docosahexaenoic acid (DHA), an omega-3 fatty acid, is involved in memory, synaptic membrane biogenesis and function, and neuroprotection (Bazan, 2006). DHA is the precursor of novel mediators, including resolvins and protectins, in resolving inflammatory exudates (Serhan et al., 2002). One of the protectins, 10,17-docosatriene, is produced in murine ischemic stroke and is a potent regulator of polymorphonuclear neutrophil (PMN) infiltration, reducing stroke-mediated tissue damage (Marcheselli et al., 2003; Serhan et al., 2002). Given its potent protective actions in the retina and brain, we initially termed this DHA-derived mediator neuroprotectin D1 (NPD1) (Bazan et al., 2010; Mukherjee et al., 2004; Stark and Bazan, 2011a). Recently, we reported discovery of novel aspirin-triggered DHA metabolome, a potent anti-inflammatory proresolving molecule, namely aspirin-triggered Neuroprotectin D1 (AT-NPD1, 10R, 17R–dihydroxy-docosa-4Z,7Z,11E,13E,15Z,19Z-hexaenoic acid) (Serhan et al., 2011). We demonstrated that AT-NPD1 treatment reduced PMN recruitment in murine peritonitis, decreased transendothelial PMN migration as well as enhanced efferocytosis of apoptotic human PMN by macrophages (Serhan et al., 2011). Since DHA is released from membrane phospholipids, we asked if novel COX-2-derived DHA bioactive derivatives are formed during brain ischemic reperfusion in the presence of DHA plus aspirin.

The present study was designed to identify a novel biosynthetic pathway that leads to the formation of AT-NPD1, when DHA plus aspirin is administered after stroke. In addition, we investigated whether administration of synthetic AT-NPD1 in either its sodium salt or as the methyl ester is able to salvage ischemic penumbra. We used magnetic resonance imaging (MRI) and lipidomic analysis in conjunction with behavioral, histological, and immunostaining methods to understand this novel therapeutic approach.

Materials and methods

Animal preparation

All studies were approved by the Institutional Animal Care and Use Committee of the Louisiana State University Health Sciences Center. Male Sprague-Dawley rats, weighing 279-340 g (Charles River Lab., Wilmington, MA), were used in all studies. Atropine sulfate (0.5 mg/kg, i.p.) was injected 10 minutes before anesthesia. Anesthesia was induced with 3% isoflurane in a mixture of 70% nitrous oxide and 30% oxygen. All rats were orally intubated and mechanically ventilated. During ventilation, the animals were paralyzed with pancuronium bromide (0.6 mg/kg, i.p.). Temperature probes were inserted into the rectum and the left temporalis muscles. Heating lamps were used to maintain temperatures at 36° to 37°C during and after surgical procedures. The right femoral artery and vein were catheterized for blood sampling for arterial gases, pH, plasma glucose, and drug infusion.

Transient MCAo model

The right middle cerebral artery (MCA) was temporarily occluded for 2 hour by an intraluminal-filament, coated with poly-L-lysine, as previously described (Belayev et al., 1996). Briefly, the right common carotid artery (CCA) was exposed through a midline neck incision and dissected free of the surrounding nerves; the occipital branches of the external carotid artery (ECA) were coagulated, and the pterygopalatine artery was ligated. A 4-cm length of 3-0 monofilament nylon suture was inserted via the proximal ECA into the internal carotid artery (ICA) and MCA a distance of 20-22 mm from the CCA bifurcation, according to the animal's weight. Following suture placement, the neck incision was closed, animals were allowed to awaken from anesthesia, and then they were tested on a standardized neurobehavioral battery. After 2 hours of MCAo, rats were reanesthetized with the same anesthetic combination. Temperature probes were reinserted, intraluminal sutures were carefully removed, and the animals were allowed to survive for 24 hours or 7 days according to experimental design with free access to food and water.

Behavioral Tests

Behavioral tests were performed by an observer blinded to the treatment groups at 60 minutes (during MCAo) and then on days 1, 2, 3 and 7 after MCAo. The battery consisted of two tests that have been used previously (Belayev et al., 1996) to evaluate various aspects of neurologic function: (1) the postural reflex test, to examine upper body posture while the animal is suspended by the tail, and (2) the forelimb placing test, to examine sensorimotor integration in forelimb placing responses to visual, tactile and proprioceptive stimuli. Neurological function was graded on a scale of 0 (normal) to 12 (maximal injury) as we previously described (Belayev et al, 1996). Only animals with a high-grade neurological deficit (10 or greater) were used in this study.

Treatment and study protocols

Animals were treated with aspirin, DHA or a combination of both. The vehicle group received a comparable volume of 0.9% sodium chloride. Synthetic AT-NPD1-SS and AT-

NPD1-ME were prepared in stereochemically-pure form via total organic synthesis (Serhan et al, 2011). In each series described below, rats underwent 2 hours of MCAo.

In series 1, animals were treated with aspirin (30 mg/kg, i.p., 30 minutes before MCAo), DHA (5 mg/kg, i.v., at 3 hours from MCAo onset) or combination of both drugs, followed by lipidomic analysis at 24 hours. In series 2, animals were treated with AT-NPD1 (333 μg/kg) in either sodium salt (AT-NPD1-SS) or as methyl ester (AT-NPD1-ME) and saline (n=7-8). Behavioral testing were conducted on days 1, 2, 3 and 7 followed by magnetic resonance imaging (MRI) and immunohistochemistry on day 7.

Ex vivo MRI data collection and analysis

High resolution e*x vivo* MRI data were acquired from 4% paraformaldehyde (PFA) fixed brains on day 7 using an 11.7T Bruker Advance 8.9 cm horizontal bore instrument equipped with a 89 mm (ID) receiver coil (Bruker Biospin, Billerica, MA) as previously described (Sun et al, 2003). MRI-derived lesion volumes were extracted from high resolution T2 weighted images (T2WI) and encompassed cortical and subcortical regions of the entire brain, from which 3D reconstructions were generated to illustrate the extent of the lesions. T2 and diffusion tensor imaging (DTI) were performed to a) extract quantitative MR values, including tissue T2 relaxation and water mobility (ADC) from cortical and subcortical regions, and b) quantitate directional water mobility from the corpus callosum (CC) extracting measures of white matter integrity, including relative anisotropy, axial diffusivity (mm^2/sec), radial diffusivity (mm^2/sec) and trace (equivalent to mean diffusivity, mm^2/sec).

Lipidomic analysis

Lipidomic analysis was conducted as previously described (Bazan, et al., 2008). Rats were perfused with cold ice saline at 1 day after stroke. For each animal, the brain was removed and blocked into two segments that included the bregma levels +2.7 and −0.3 mm. Next, coronal blocks were divided into right and left hemispheres and cut into two regions (one for cortex and one for striatum). The brain samples were immediately frozen in liquid nitrogen and then homogenized in cold methanol. Purification was performed by solid-phase extraction technique. In short, samples pre-equilibrated at pH 4.0 were loaded onto C18 columns (Varian) and eluted with 10 ml methanol. Samples were concentrated by a nitrogen stream evaporator before LC-MS analysis. Samples were analyzed using TSQ Quantum Ultra UPLC-MS/MS triple stage tandem mass spectrometer from Thermo Electronic Company, Inc., at SRM mode. The samples were injected and eluted through a reversed phase Eclipse Plus C18 column (4.6×75mm, 1.8μm) from Agilent Technologies with a flow rate of the mobile phase at 400 μL/min driven by an Accela pump. The elutant was detected by the mass spectrometer. The runs started with the mobile phase of B (H_2O:Acetic acid=100:0.01):D (Methanol:Acetic acid=100:0.01) =70:30 to 100% D in 12 minutes, followed by 100% D for 6 minutes, then returned to B:D=70:30 and kept for 5 minutes. 17S-Hydroxyl DHA (17S-HDHA) and 17R-HDHAwere separated by CHIRALPAK IA chiral column (2 mm ×150 mm, 5.0 μm particle size). The column was eluted at 100 μL/minutes by Mobile phase mixed from B and C (Acetonitrile:acetic acid = 100:0.01) in the following linear gradient. It started from [15% B + 85% C] at 0 min, ramped to [10% A + 90% C] at 10 min, then ramped to [100% C] at 15 min and stayed at 100% C for 8 min, then went back to [15% B + 85% C] at 27 min. The mass spectrometer was set at a spray voltage of 3100 V, vaporizer temperature at 380°C, sheath gas pressure at 40 psi, auxiliary gas pressure at 2 psi, capillary temperature at 245°C, and collision pressure at 1.5 mTorr. The SRM chromatographs of samples were compared with those of standards of DHA (327.2→283.2), 17-hydroxyl DHA (343.2→245.0), NPD1 (359.2→153) and AT-NPD1 (359.2→153), and PGE_2 (351.2→189.1) with the same retention times. AT-NPD1 came out of the column at 7.35 minutes, which was earlier than NPD1 at 8.07 minutes. PGD2-d_4 was used as the

internal standard for NPD1, AT-NPD1, and PGE2; EPA-d_5 was used as the internal standard for DHA and 17-hydroxyl DHA.

Histopathology

Animals were perfused with 4% paraformaldehyde on day 7, and brains were removed and embedded in a gelatin matrix using MultiBrain™ Technology (NeuroScience Associates, Knoxville, TN) as previously described (Thompson et al, 2006). Coronal sections were stained with thionine (Nissl), digitized at nine standardized coronal levels, and the area of infarction was measured and analyzed using MCID™ Core imaging software (Linton, Cambridge, United Kingdom) as previously described (Belayev et al, 1996). An investigator blinded to the experimental groups then outlined the zones of infarction (which were clearly demarcated) as well as the left and right hemispheres of each section. Infarct volume was calculated as the integrated product of cross-sectional area and inter-section distance and corrected for brain swelling.

Immunostaining

Immunohistochemical procedures were performed on the adjacent sections to identify specific vascular and neuronal elements in the ischemic core and penumbra. The following antibodies were used: rat blood-brain barrier (SMI-71, Sternberger Monoclonals, Inc., Baltimore, MD) as a vascular marker, glial fibrillary acid protein (GFAP, Santa Cruz, SDS Biosciences, Sweden) to label reactive astrocytes, and Cd68/ED-1 (Serotec, Raleigh, NC) for activate microglia/macrophages. Numbers of GFAP, ED1 and SMI-71 immunopositive vessels were counted in the three cortical and one subcortical area (ipsi- and contralateral sides) at the level of the central lesion (bregma level -0.3 mm). Data were expressed as numbers of positive cells and vessels per high-power microscopic field (magnification X 40). Brain slices were imaged on a Zeiss LSM-510 Meta laser confocal microscope with a 10× objective (Zeiss Plan-NEOFLUAR 10×/0.3; Carl Zeiss MicroImaging GmbH, Germany). Computer-generated MosaiX processed images of Nissl, GFAP, ED-1 and GFAP/ED-1 double staining from saline and DHA rats were generated. Fluorophore visualization (excitation/emission capture) was achieved as follows: GFAP (astrocytes): Dylight 488 (488 nm/505-530 nm, green) and ED1 (microglia): Dylight 594 (594 nm/ 603-636 nm, red). Image resolution was set to 2.26 μm/pixel and the cubic voxel dimension was 129.5 μm.

Statistical analysis

Data are presented as mean values ± s.e.m. Repeated measures analysis of variance (ANOVA) followed by Bonferroni procedures (to correct for multiple comparisons) were used for intergroup comparisons of neurobehavioral scores over time and infarct areas across coronal levels. Two-tailed Student's *t* tests were used for two-group comparisons. Differences at $P<0.05$ were considered statistically significant.

Results

Physiological variables

Rectal and cranial (temporalis muscle) temperatures, arterial blood gases, and plasma glucose showed no significant differences between animals (Table 1). There were no adverse behavioral side effects observed after aspirin, DHA, or AT-NPD1 administration to rats in all groups. No animals died during this study.

Aspirin plus DHA treatment induces endogenous brain biosynthesis of AT-NPD1

Liquid chromatography–photodiode array detection–electrospray ionization–tandem mass spectrometry (LC-PDA-ESI-MS/MS)-based mediator lipidomic analysis of contralateral and ipsilateral brain regions demonstrated AT-NPD1 in the ipsilateral side following aspirin plus DHA treatment, but not with either aspirin or DHA alone (Fig. 1A). Our results confirm that NPD1 biosynthesis is induced during ischemia-reperfusion after DHA treatment (Fig. 1B). As expected, PGE_2 was reduced by aspirin; aspirin plus DHA treatments also reduced the content of PGE_2 (Fig. 1C).

NPD1 and AT-NPD1 in the ipsilateral side after MCAo were obtained by matching the liquid chromatography-tandem mass spectrometry (LC-MS/MS) chromatograms and spectrum to authentic synthetic compounds (Fig. 1D-F). The multiple reaction monitoring (MRM) chromatogram at m/z 359 > (m/z 153, 206) showed that more bioactive AT-NPD1 was generated within the penumbral tissues following of aspirin plus DHA administration (Fig, 1D,E). The MS/MS ions m/z 359[M-H]-, 341[M-H-H_2O]-, 323[M-H-H_2O_2]-, 315[M-H-CO_2]-, 297[M-H-H_2O-CO_2]-, 261, 243 [261-H_2O]-, 217[261-CO_2]-, 206, and 153 were consistent with one carboxyl, two hydroxyls, and the molecular weight (M) of AT-NPD1 and NPD1, which was 360, as well as the positions of the hydroxyl groups (Fig. 1E). We also found 17*R*-HDHA, a reduced product of AT-NPD1-precursor 17R-HpDHA, as a marker for the biosynthetic pathway of AT-NPD1 (Fig. 1 G) (Serhan et al, 2011). Moreover, we confirmed the formation of 17S-HDHA (Fig. 1 G), the reduced product of 17S-hydroperoxy-docosahexaenoic acid (17S-HpDHA) and an intermediate of NPD1 biosynthesis in human cells (Marcheselli et al., 2003), as shown by chiral-LC selected reaction monitoring (SRM) chromatogram at m/z 343 > 245, respectively (Fig 1G).

AT-NPD1 induces sustained neurological improvement

We undertook the total organic chemical synthesis of stereochemically pure AT-NPD1 (Serhan et al, 2011) to evaluate whether these novel molecules could improve behavioral deficits. Intravenous administration of AT-NPD1-SS or AT-NPD1-ME at 3 hours after stroke onset greatly improved neurological status in a sustained fashion up to the 7-day period studied (Fig. 2A). Saline-treated animals continued to exhibit severe impairments throughout this period. Both AT-NPD1 groups had remarkably improved time courses for recovery of postural reflexes, proprioceptive and tactile contralateral forelimb reactions at days 1-7 (Fig. 2B-E).

AT-NPD1 reduces lesion volumes, brain edema and improves water mobility

Analysis of lesion volumes at day 7 found that treatment with AT-NPD1 alone, used either as its sodium salt or as its carboxyl methyl ester, significantly reduced cortical, subcortical and total infarct areas and volumes (Fig. 3A-C). The AT-NPD1-SS treated group had smaller lesion volumes that were visible only in a small portion of the cortex and subcortical areas (Fig. 3D). In contrast, AT-NPD1-ME treated rats had lesions primarily located only in a small portion of the striatum (Fig. 3D). It is tempting to suggest that this more potent effect of AT-NPD1-ME might be due to a pro-drug nature resulting from the presence of the methyl group, which provides accessibility and longer availability than AT-NPD1-SS. Treatment with AT-NPD1-SS decreased brain edema within the cortex and subcortex and water mobility (ADC) was reduced only in the cortex (Fig. 3E,F). Three-dimensional lesion volumes were dramatically reduced by both AT-NPD1 treatments, compared to saline-treated rats, which showed large cortical and subcortical lesion volumes (Fig. 3G).

AT-NPD1 protects white matter

Diffusion anisotropy, as measured by relative anisotropy (RA), is sensitive to alterations in white matter fiber integrity (Le Bihan et al, 2001) and has been used successfully to detect subtle abnormalities after stroke [RA=1/fractional anisotropy (FA)]. We demonstrated here that the RA within the CC of saline-treated animals was decreased and that treatment with AT-NPD1-ME results in a return to normative RA values (0.64) (Fig. 4A,B). A significant difference in RA was found between saline and AT-NPD1-ME-treated animals, while AT-NPD1-SS treated animals showed a non-statistical trend towards neuroprotection. Measures of axial (axonal), radial (myelin) and mean (apparent diffusion coefficient, ADC) diffusivity were obtained, but no significant differences were observed in the DTI measures of white matter integrity at the 7d timepoint.

AT-NPD1 attenuates histological brain damage

Focal cerebral ischemia consists of an infarction (or “core”) and a variable rim of selective neuronal damage (a “histologic” penumbra). The area peripheral to the lesion core, the penumbra, is characterized by minimal histological changes (such as eosinophilic neurons) and also by an increased number of apoptotic neurons and glial cells (Mogoantă et al, 2010). Without reperfusion, the penumbra progressively deteriorates within a few hours, becoming an extension of the ischemic core. We asked if the novel AT-NPD1 could rescue the penumbra at 3h after onset of MCAo. Histologically, the brains of saline-treated animals, studied after seven days of survival, confirmed large zones of infarction involving the frontoparietal neocortex and underlying caudoputamen (Fig. 4C). These infarcted regions showed pancellular damage as well as denser areas of eosinophilic, shrunken neurons along the infarct margin. In contrast, treatment with both AT-NPD1 compounds showed markedly smaller cortical infarcts and reduced zones of basal-ganglionic infarct (Fig. 4C). Maximal protection was found within the cortex (represent penumbral area) and also in subcortical areas (Fig. 4D). In addition, both AT-NPD1 treatments reduced total infarct volumes and areas at multiple coronal levels (Fig. 4D).

AT-NPD1 attenuates cellular damage and blood vessel integrity

Macrophages, astrocytes and blood vessels implicated in cerebral infarction were examined using immunohistochemistry on day 7. Saline-treated rats exhibited lesions involving large cortical and subcortical regions, characterized by loss of neuronal, glial, vascular elements and massive ED-1-positive microglia/macrophage infiltration (Fig. 5A). Cellular counts for SMI-71, GFAP, ED-1 (regions delineated in Fig 5B) demonstrated that both AT-NPD1 treatments attenuated tissue loss, decreased ED-1-positive microglia/macrophages, and protected blood vessel integrity and GFAP-positive reactive astrocytes (Fig. 5C-E). As a result of AT-NPD1 treatments, blood vessel density increased within the penumbral tissues, with parallel formation of a denser GFAP-rich scar tissue. Thus, enhancement of blood vessel density likely facilitates neurogenesis and synaptogenesis, which in turn contributes to improved repair and, ultimately, improved functional recovery.

Discussion

The present study had two main goals: 1) to identify a novel biosynthetic pathway that leads to the formation of AT-NPD1 mediator, and 2) to evaluate whether administration of synthetic AT-NPD1 in either its sodium salt or as the methyl ester is able to salvage the ischemic penumbra.

We identified a novel biosynthetic pathway that leads to the formation of AT-NPD1 mediator, when aspirin plus DHA are administered after stroke. AT-NPD1 displays a 17*R*-stereochemistry (Marcheselli et al., 2003; Serhan et al., 2011; Serhan et al, 2002), unlike the

17*S* chirality displayed in NPD1, which is produced via a lipoxygenase reaction (Marcheselli et al., 2003; Serhan et al., 2006). In the central nervous system, COX-2 is abundantly and constitutively expressed and is involved both in normal functions as well as pathology (Kaufmann et al., 1996; Stark and Bazan, 2011a; Stark and Bazan, 2011b; Tu and Bazan, 2003). Since the COX-2 catalytic site is larger than that of COX-1, its aspirin-induced acetylation does not result in complete inhibition. Instead, aspirin-acetylated COX-2 converts arachidonic acid to 15R-hydroxyeicosatetraenoic acid (15R-HETE), a lipoxygenase-like product having and R- rather than the typical S- chirality (Clària and Serhan, 1995; Rowlinson et al., 2000). 15R-HETE is converted then to potent anti-inflammatory aspirin-triggered 15-epi lipoxins that retain the C-15 hydroxyl group in the *R* configuration (Chiang et al., 2004; Takano et al., 1997). Aspirin acetylation of COX-2 gives rise to catalytic activity that converts DHA to 17*R*-hydroxy products, one of which was first identified in the resolution phase of inflammatory exudates and brain tissues of mice treated with aspirin. This product's basic structure was proposed previously (Marcheselli et al., 2003; Serhan et al., 2002) and the complete structure and stereochemistry of this DHA-derived lipid mediator was recently elucidated to be AT-NPD1 (Serhan et al, 2011). The chirality of carbon-10 and -17 hydroxyl groups and the geometry of the conjugated triene unit, which are essential for the potent bioactivity of this aspirin-triggered omega-3 fatty acid lipid mediator, were established by matching it with pure materials prepared unambiguously by total organic synthesis (Serhan et al, 2011).

We also employed MRI, a highly sensitive tool for the detection of changes in water content and diffusion that characterize acute ischemic stroke. The rapid induction of brain edema following focal ischemia is a leading cause of morbidity and death after stroke. Neuroimaging of the penumbra is a strategy for detecting tissue at risk (Donnan et al., 2009), especially when up to 44% of patients may still retain penumbral tissue 18 hours after stroke (Ebinger et al., 2009). We have shown here that synthetic AT-NPD1, delivered at 3 hours after stroke onset, reduces brain lesion and edema and improves tissue matrix (ADC). In addition, treatment with AT-NPD1-ME after stroke significantly enhanced and protected white matter in our studies. In humans and experimental models of stroke, the change of diffusion anisotropy within the ischemic area discloses the degree of structural damage within the white matter and provides indices of functional potential (Li et al., 2009). *Ex vivo* DTI have been shown to be equivalent to *in vivo* DTI (Sun et al., 2003). Treatment with AT-NPD1-ME after stroke significantly enhanced and protected white matter, which likely underlies the observed improvements in neurological function. It is possible that the methyl ester form of AT-NPD1 might have a longer half-life, resulting in increased duration of sustained bioactivity needed for neuroprotection.

Cerebral ischemia initiates a complex cascade of cellular, molecular and metabolic events that lead to irreversible brain damage (Iadecola and Anrather, 2011; Moskowitz et al, 2010; Ratan, 2010). As the infarct progresses, the neurovascular lesions worsen (Mogoantă et al, 2010). Dead neurons and injured tissue are scavenged by activated resident microglia and/or macrophages that invade the injured tissue from the blood stream. Surviving astrocytes and activated microglia in the penumbra may facilitate restoration of neuronal integrity by producing growth factors, cytokines, and extracellular matrix molecules involved in repair mechanisms (Panickar and Norenberg, 2005). PMN infiltration and resolution are therapeutic targets, since protective PMNs (i.e., acute inflammatory responses) are programmed to be self-limited and tightly controlled in brain ischemic-reperfusion damage (Marcheselli et al, 2003). Our novel results demonstrate that AT-NPD1 is endogenously produced in the stroke-injured brain upon aspirin plus DHA treatment. Maximal protection was detected in the cortex (the penumbral area) and also in subcortical area. Smaller infarcts with less pancellular damage, denser areas of eosinophilic, and shrunken neurons along the infarct margin were detected in all AT-NPD1treated rats. AT-NPD1-SS and AT-NPD1-ME

treated rats reduced the total infarct volumes by 69% and 84%, respectively. Both AT-NPD1 treatments decreased ED-1-positive microglia/macrophages and also increased blood vessel density in the penumbra, with parallel formation of a denser GFAP-rich scar tissue. The integrity of blood vessels facilitates neurogenesis and synaptogenesis, which in turn contributes to improved functional recovery.

Focal ischemic stroke leads to impaired sensorimotor and cognitive functions with 70-80% of patients displaying hemiparesis immediately after stroke. Functional deficits in rodents following MCAo resemble sensorimotor deficits. Since the ultimate goal of any stroke therapy is the restoration of behavioral functions, two tests of the sensorimotor battery were used to detect neurological deficits following experimental stroke. Both AT-NPD1 treatments improved overall neurological recovery highlighted by the time course of recovery of postural reflex, and proprioceptive and tactile contralateral forelimb reactions through the 7-day survival period.

In summary, we have shown neuroprotection by AT-NPD1, a novel endogenous DHA-derived lipid mediator generated via aspirin-acetylated COX-2. We also demonstrated the *in vivo* biosynthesis of AT-NPD1 in the ipsilateral side following DHA plus aspirin treatment during brain ischemia-reperfusion. Also, we have shown that synthetic AT-NPD1, delivered at 3 hours after stroke onset, provides sustained neurobehavioral recovery, reduces brain infarction and brain edema, improves tissue matrix (ADC), and protects white matter. In some instances, AT-NPD1-ME was more effective than AT-NPD1 dissolved in sodium salt, possibly due to its longer half-life. The novel AT-NPD1 endogenous pathway may provide the basis for pharmaceutical development and clinical translation for the treatment of ischemic stroke.

Acknowledgments

This work was supported in part by National Institutes of Health (NIH, Bethesda, MD), National Center for Complementary and Alternative Medicine grant RC2 AT005909 (N.G.B., C.N.S., N.A.P.). We thank Sonny Kim and Kamalakar Ambadipudi for MRI acquisition and analysis assistance, and Neuroscience Associates, Inc. for histology service.

References

Bazan NG. Cell survival matters: docosahexaenoic acid signaling, neuroprotection and photoreceptors. Trends Neurosci. 2006; 29:263–271. [PubMed: 16580739]

Bazan NG. Omega-3 fatty acids, pro-inflammatory signaling and neuroprotection. Curr Opin Clin Nutr Metab Care. 2007; 10:136–141. [PubMed: 17285000]

Bazan, NG.; Marcheselli, VL.; Lu, Y.; Hong, S.; Jackson, F. Lipidomic approaches to neuroprotection signaling in the retinal pigement epithelium. In: Fliesler, SJ.; Kisselev, OG., editors. Signal Transduction in the Retina. CRC Press; 2008. p. 349-373.

Bazan NG, Calandria JM, Serhan CN. Rescue and repair during photoreceptor cell renewal mediated by docosahexaenoic acid-derived neuroprotectin D1. J Lipid Res. 2010; 51:2018–2031. [PubMed: 20382842]

Belayev L, Alonso OF, Busto R, Zhao W, Ginsberg MD. Middle cerebral artery occlusion in the rat by intraluminal suture. Neurological and pathological evaluation of an improved model Stroke. 1996; 27:1616–1622.

Chiang N, Bermudez EA, Ridker PM, Hurwitz S, Serhan CN. Aspirin triggers anti-inflammatory 15-epi-lipoxin A4 and inhibits thromboxane in a randomized human trial. Proc Natl Acad Sci USA. 2004; 101:15178–15183. [PubMed: 15471991]

Clària J, Serhan CN. Aspirin triggers previously undescribed bioactive eicosanoids by human endothelial cell-leukocyte interactions. Proc Natl Acad Sci USA. 1995; 92:9475–9479. [PubMed: 7568157]

Donnan GA, Fisher M, Macleod M, Davis SM. Stroke. Lancet. 2008; 371:1612–23. [PubMed: 18468545]

Donnan GA, Baron JC, Ma H, Davis SM. Penumbral selection of patients for trials of acute stroke therapy. Lancet Neurol. 2009; 8:261–269. [PubMed: 19233036]

Ebinger M, De Silva DA, Christensen S, Parsons MW, Markus R, Donnan GA, Davis SM. Imaging the penumbra - strategies to detect tissue at risk after ischemic stroke. J Clin Neurosci. 2009; 16:178–187. [PubMed: 19097909]

Iadecola C, Anrather J. The immunology of stroke: from mechanisms to translation. Nat Med. 2011; 17:796–808. [PubMed: 21738161]

Kakar P, Watson T, Lip GY. New approaches to therapy with omega-3 fatty acids. Curr Atheroscler Rep. 2008; 10:79–87. [PubMed: 18366989]

Kaufmann WE, Worley PF, Pegg J, Bremer M, Isakson P. COX-2, a synaptically induced enzyme, is expressed by excitatory neurons at postsynaptic sites in rat cerebral cortex. Proc Natl Acad Sci USA. 1996; 93:2317–2321. [PubMed: 8637870]

Le Bihan D, Mangin JF, Poupon C, Clark CA, Pappata S, Molko N, Chabriat H. Diffusion tensor imaging: concepts and applications. J Magn Reson Imaging. 2001; 13:534–546. [PubMed: 11276097]

Li L, Jiang Q, Ding G, Zhang L, Li Q, Panda S, Kapke A, Lu M, Ewing JR, Chopp M. MRI identification of white matter reorganization enhanced by erythropoietin treatment in a rat model of focal ischemia. Stroke. 2009; 40:936–941. [PubMed: 19150870]

Lo EH. A new penumbra: transitioning from injury into repair after stroke. Nat Med. 2008; 14:497–500. [PubMed: 18463660]

Marcheselli VL, Hong S, Lukiw WJ, Tian XH, Gronert K, Musto A, Hardy M, Gimenez JM, Chiang N, Serhan CN, Bazan NG. Novel docosanoids inhibit brain ischemia-reperfusion-mediated leukocyte infiltration and pro-inflammatory gene expression. J Biol Chem. 2003; 278:43807–43817. [PubMed: 12923200]

Mogoantă L, Pirici D, Pop OT, Bălşeanu AT, Rolea E, Dahnovici RM. Study of vascular microdensity in areas of cerebral ischemia on experimental model. Rom J Morphol Embryol. 2010; 51:725–731. [PubMed: 21103633]

Moskowitz MA, Lo EH, Iadecola C. The science of stroke: mechanisms in search of treatments. Neuron. 2010; 67:181–198. [PubMed: 20670828]

Mukherjee PK, Marcheselli VL, Serhan CN, Bazan NG. Neuroprotectin D1: a docosahexaenoic acid-derived docosatriene protects human retinal pigment epithelial cells from oxidative stress. Proc Natl Acad Sci USA. 2004; 101:8491–8496. [PubMed: 15152078]

Panickar KS, Norenberg MD. Astrocytes in cerebral ischemic injury: morphological and general considerations. Glia. 2005; 50:287–298. [PubMed: 15846806]

Ratan RR. Beyond neuroprotection to brain repair: exploring the next frontier in clinical neuroscience to expand the therapeutic window for stroke. Transl Stroke Res. 2010; 1:71–73. [PubMed: 20539747]

Rowlinson SW, Crews BC, Goodwin DC, Schneider C, Gierse JK, Marnett LJ. Spatial requirements for 15-(R)-hydroxy-5Z,8Z,11Z,13E-eicosatetraenoic acid synthesis within the cyclooxygenase active site of murine COX-2. J Biol Chem. 2000; 275:6586–6591. [PubMed: 10692466]

Schwab JM, Chiang N, Arita M, Serhan CN. Resolvin E1 and protectin D1 activate inflammation-resolution programmes. Nature. 2007; 447:869–874. [PubMed: 17568749]

Serhan CN, Hong S, Gronert K, Colgan SP, Devchand PR, Mirick G, Moussignac RL. Resolvins: a family of bioactive products of omega-3 fatty acid transformation circuits initiated by aspirin treatment that counter pro-inflammation signals. J Exp Med. 2002; 196:1025–1037. [PubMed: 12391014]

Serhan CN, Gotlinger K, Hong S, Lu Y, Siegelman J, Baer T, Yang R, Colgan SP, Petasis NA. Anti-inflammatory actions of neuroprotectin D1/protectin D1 and its natural stereoisomers: assignments of dihydroxy-containing docosatrienes. J Immunol. 2006; 176:1848–1859. [PubMed: 16424216]

Serhan CN, Fredman G, Yang R, Karamnov S, Belayev LS, Bazan NG, Zhu M, Winkler JW, Petasis NA. Novel proresolving aspirin-triggered DHA pathway. Chem Biol. 2011; 18:976–987. [PubMed: 21867913]

Stark DT, Bazan NG. Neuroprotectin D1 induces neuronal survival and downregulation of amyloidogenic processing in Alzheimer's disease cellular models. Mol Neurobiol. 2011a; 43:131–138. [PubMed: 21431475]

Stark DT, Bazan NG. Synaptic and extrasynaptic NMDA receptors differentially modulate cyclooxygenase-2 function, lipid peroxidation, and neuroprotection. J Neurosci. 2011b; 31:13710–13721. [PubMed: 21957234]

Sun SW, Neil JJ, Song SK. Relative indices of water diffusion anisotropy are equivalent in live and formalin-fixed mouse brains. Magn Reson Med. 2003; 50:743–748. [PubMed: 14523960]

Takano T, Fiore S, Maddox JF, Brady HR, Petasis NA, Serhan CN. Aspirin-triggered 15-epi-lipoxin A4 (LXA4) and LXA4 stable analogues are potent inhibitors of acute inflammation: Evidence for anti-inflammatory receptors. J Exp Med. 1997; 185:1693–1704. [PubMed: 9151906]

Thompson SN, Gibson TR, Thompson BM, Deng Y, Hall ED. Relationship of calpain-mediated proteolysis to the expression of axonal and synaptic plasticity markers following traumatic brain injury in mice. Exp Neurol. 2006; 201:253–265. [PubMed: 16814284]

Tu B, Bazan NG. Hippocampal kindling epileptogenesis upregulates neuronal cyclooxygenase-2 expression in neocortex. Exp Neurol. 2003; 179:167–175. [PubMed: 12618123]

Yip S, Benavente O. Antiplatelet agents for stroke prevention. Neurotherapeutics. 2011; 8:475–487. [PubMed: 21761240]

Highlights

- Aspirin plus DHA treatment induces endogenous brain biosynthesis of AT-NPD1.
- We examine the effects of AT-NPD1 treatment on experimental stroke model in rats.
- AT-NPD1 improves behavior and reduces brain infarction at 7 days after stroke.
- AT-NPD1 attenuates brain edema and protects white matter.
- Treatment with AT-NPD1 may be beneficial for stroke patients.

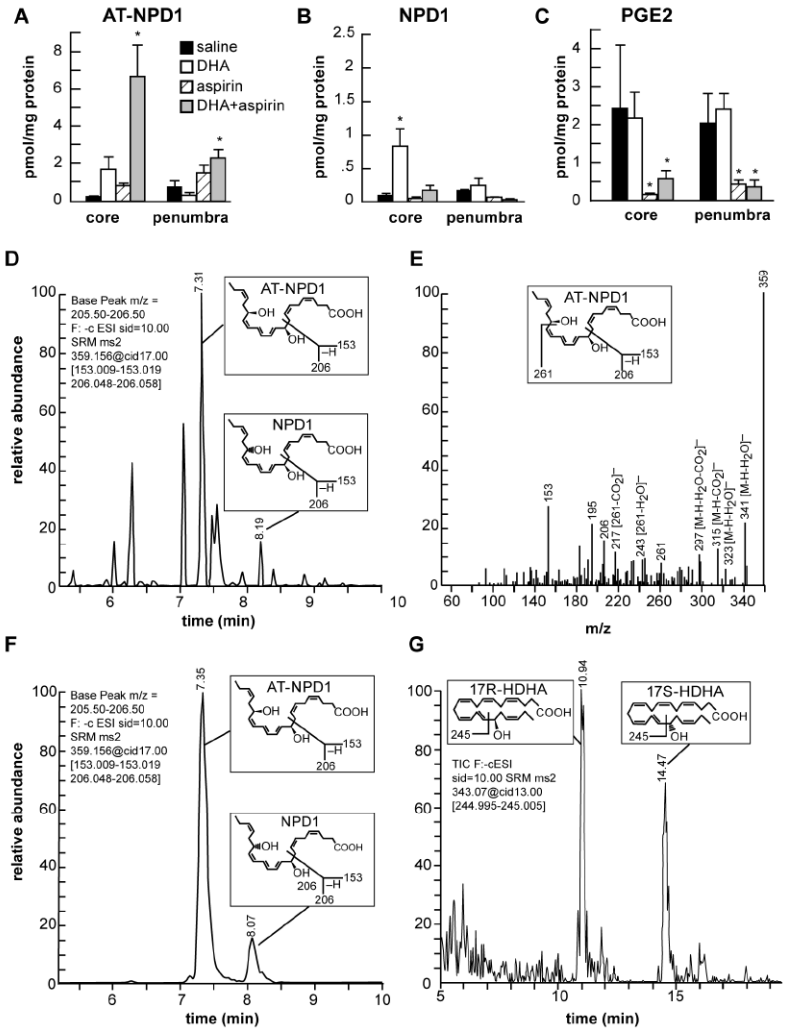

Fig. 1.

Characterization of AT-NPD1 and evidence for its biosynthesis in the ischemic brain upon systemic administration of DHA plus aspirin.

(A) AT-NPD1 synthesis was increased by DHA plus aspirin; (B) NPD1 was increased by DHA treatment; (C) PGE2 was reduced by aspirin and aspirin plus DHA treatments; (D) NPD1 and AT-NPD1, shown by a representative multiple reaction monitoring (MRM) chromatogram; (E) typical LC-MS/MS spectrum of endogenous AT-NPD1; (F) NPD1 and AT-NPD1 authentic synthetic standards shown by a MRM chromatogram; (G) 17R-HDHA and 17S-HDHA, stable derivatives of the short lived hydroperoxy precursors of AT-NPD1 and NPD1, respectively, are depicted by a representative selective reaction monitoring (SRM) chromatogram. The structure and mechanism for the generation of diagnostic mass spectrometric fragment ion for each compound are illustrated as the insert in each panel.

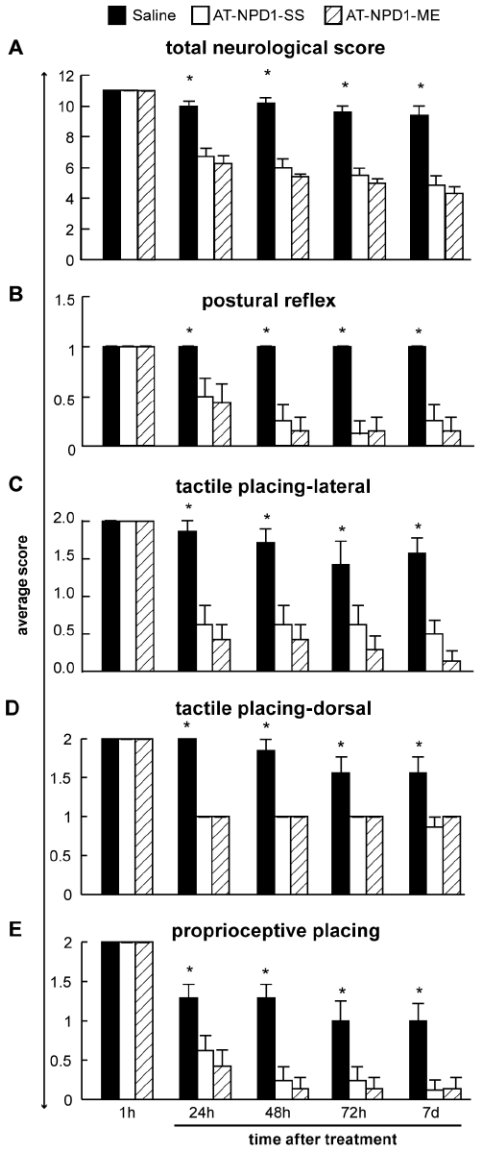

Fig. 2.

AT-NPD1 improves neurological deficit. (A) Total neurological score (normal score=0, maximal score=12) in rats during MCAo (1h) and at various survival times after MCAo. All treatments were administered iv at 3h after onset of stroke. Both AT-NPD1 treatments improved the behavioral score at 24, 48, 72 h and 7 days compared to saline group. (B,C) Time course of recovery of postural reflex, proprioceptive and tactile contralateral forelimb reactions (normal score = 0, maximal deficit = 2) following MCAo in rats. Bar graphs show improvement of postural reflex and placing reactions in both AT-NPD1-treated groups vs. saline-treated rats. Behavioral data are means ± SEM; n=6-9 per group. *, significantly different from saline-treated group (P<0.05; repeated-measures ANOVA followed by Bonferroni tests).

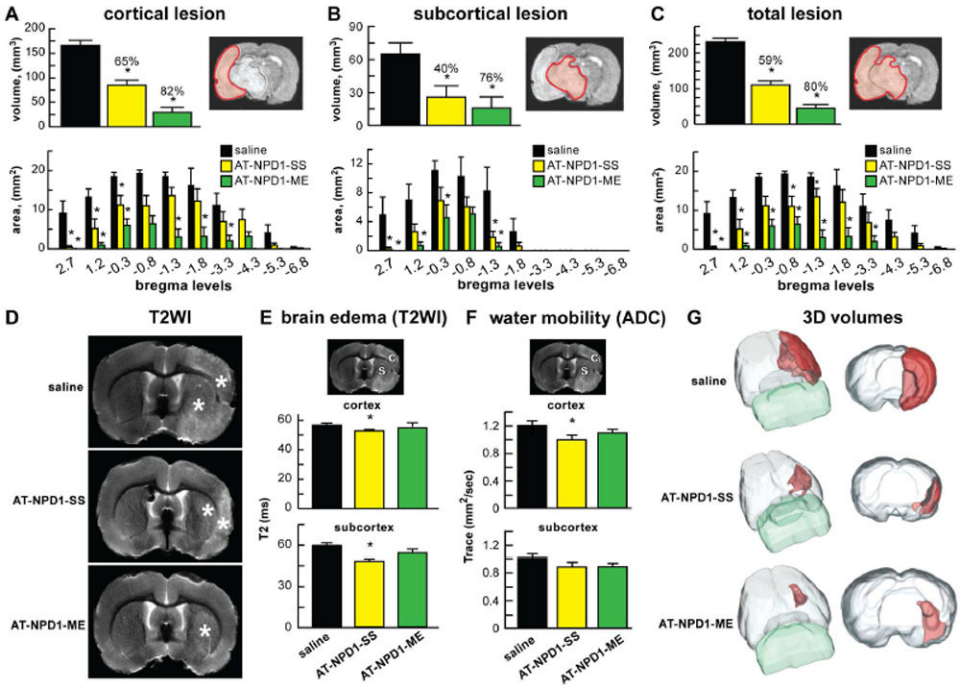

Fig. 3.

AT-NPD1 reduces lesion volumes, brain edema and improves tissue matrix. (A-C) Cortical, subcortical and total lesion areas and volumes, computed from T2WI were significantly reduced by administration of both AT-NPD1 on day 7. (D) Representative T2WI from saline, AT-NPD1-SS and AT-NPD1-ME treated rats. T2 hyperintensites were observed in the cortex and striatum of saline-treated rat, consistent with ongoing edema formation (*). AT-NPD1-SS treated animals had smaller lesion size, with only partial cortex and subcortical involvement. In contrast, AT-NPD1-ME treated rats had primarily only striatial lesions. (E) Brain edema and (F) tissue water mobility (tissue matrix, ADC) were assessed (see brain diagram for ROI: C – cortex, S - subcortex) with significant decrements in T2 and ADC in the AT-NPD1-SS group. (G) 3D lesion volumes were computed from T2WI with saline-treated rats showing large cortical and subcortical lesion volumes. A dramatic reduction in lesion volume was observed in AT-NPD1-SS that was primarily localized to small cortical and subcortical areas. In contrast, AT-NPD1-ME treatment further reduced lesion volumes that were typically only found in the striatum.

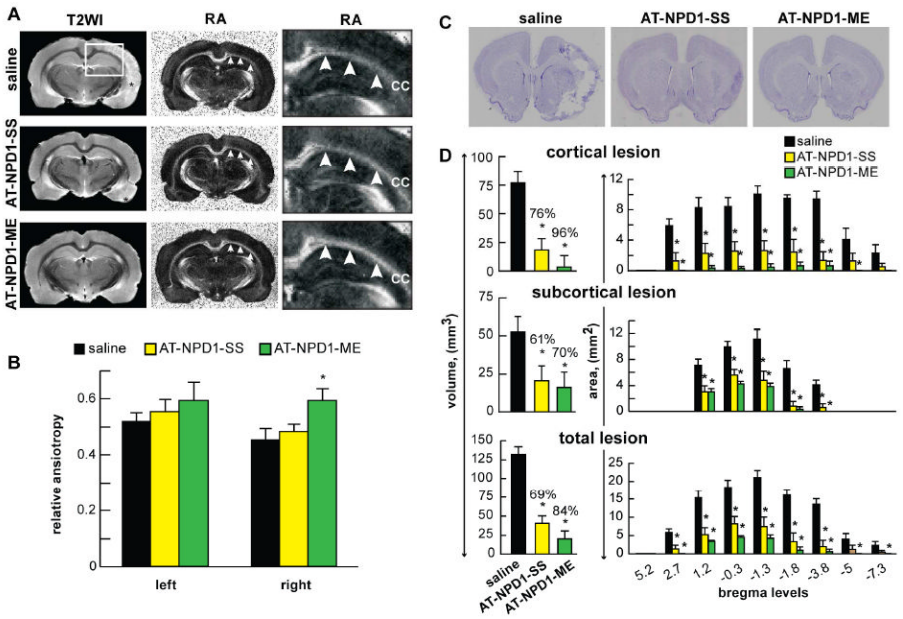

Fig. 4.

AT-NPD1-ME enhances white matter reorganization and attenuates histological brain damage. (A) Representative T2 weighted (T2WI) and relative anisotropy (RA) images reveal preservation of tissue within the corpus callosum (CC). Saline treated animals exhibited large infarct regions on T2WI (*) with a decreased lesion (*) volumes in the AT-NPD1-SS treatment group. Virtually no lesion was visible in most of the AT-NPD1-ME treated animals. RA maps demonstrated reduced CC integrity in the both the saline and AT-NPD1-SS treated animals. In contrast, treatment with AT-NPD1-ME shows an intact CC. White box on T2WI is the expanded RA region. Arrows demarcate the CC. (B) Quantitative assessment of RA values demonstrates a significant differences in RA between saline and AT-NPD1-ME treated animals (* $p<0.05$) on the side of the MCAo lesion (right). No differences were evident on the contralateral side. (C) Representative Nissl stained histology at coronal level (bregma +1.2 mm) from rats treated with saline, AT-NPD1-SS and AT-NPD1-ME at 7 days after stroke onset. A well-demarcated infarct involving cortical and subcortical regions was present in rats treated with saline. Note smaller area of cortical and subcortical infarction in rats treated with AT-NPD1-SS. In contrast, rats treated with AT-NPD1-ME had small infarction localized primarily to subcortical areas. (D) Cortical, subcortical and total infarct areas measured at 9 coronal levels and integrated infarct volumes demonstrate that treatment with both AT-NPD1 significantly reduced cortical, subcortical and total infarct areas and volumes on day 7. Results are presented as mean ± SEM; n=6-9 per group. *Significantly different from corresponding vehicle group ($p<0.05$).

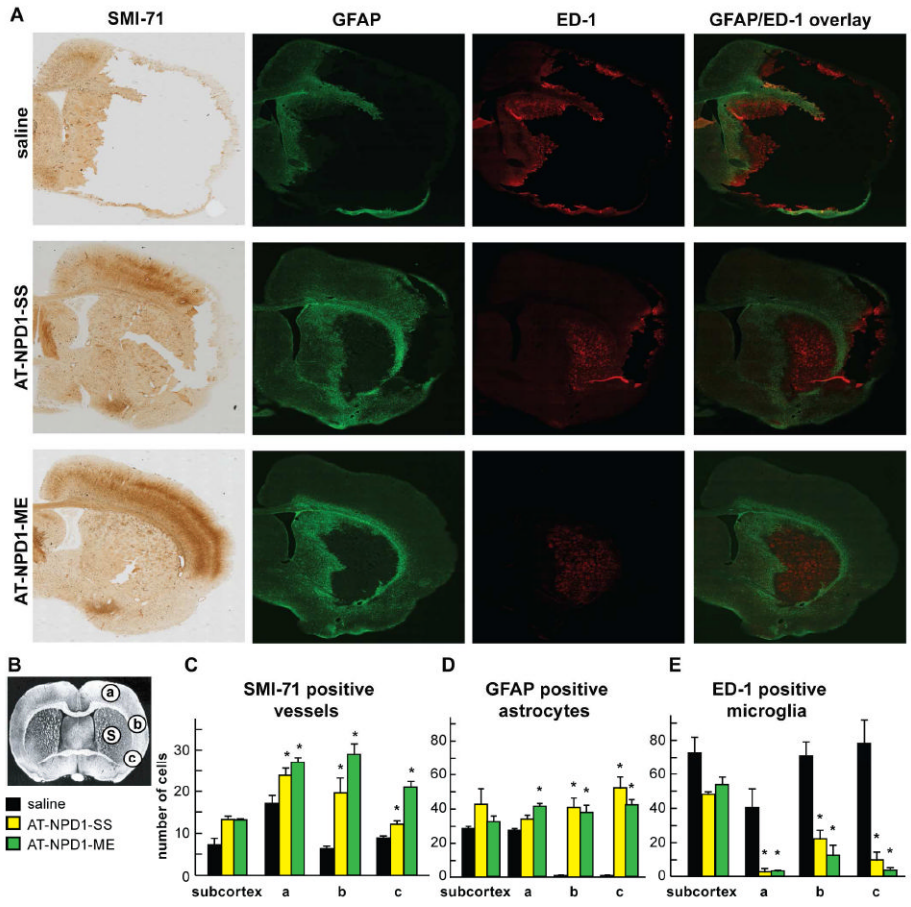

Fig. 5.

AT-NPD1 attenuates cellular damage after focal cerebral ischemia. (A) Computer-generated MosaiX processed images of SMI-71 (positive vessels), GFAP (positive astrocytes), ED-1 (positive microglia/macrophages) and GFAP/ED-1 double staining from saline, AT-NPD1-SS and AT-NPD1-ME-treated rats at a magnification 10x. All treatments were administered at 3h after onset of stroke. (B) Coronal brain diagram (bregma +1.2 mm) showing locations of regions for SMI-71, GFAP, ED-1 counts in penumbra (a, b and c) and core (C). (C-E) AT-NPD1-SS and AT-NPD1-ME increased SMI-71 positive vessels and GFAP positive astrocytes and decreased ED-1 microglia/macrophages cell count. Data are mean values ± SEM; n=6-9 per group *, significantly different from saline ($P<0.05$; repeated-measures ANOVA followed by Bonferroni tests).

Table 1

Physiological Variables

	saline (n=7)	AT-NPD1-SS (n=8)	AT-NPD1-ME (n=7)
15 min before MCAo			
rectal temperature (°C)	37.4 ± 0.06	37.1 ± 0.11	37.3 ± 0.13
cranial temperature (°C)	37.0 ± 0.10	36.6 ± 0.08 *	36.9 ± 0.17
pH	7.45 ± 0.02	7.43 ± 0.01	7.43 ± 0.01
PO2, mm Hg	112 ± 7	105 ± 4	110 ± 10
PCO2, mm Hg	38 ± 1	40 ± 1	40 ± 1
plasma glucose, mg/dL	203 ± 6	213 ± 18	148 ± 15
hematocrit, %	44 ± 1	44 ± 1	43 ± 1
body weight (g)	325 ± 15	328 ± 12	314 ± 5
15 min after MCAo			
rectal temperature (°C)	37.5 ± 0.13	37.5 ± 0.13	37.6 ± 0.07
cranial temperature (°C)	36.9 ± 0.10	36.8 ± 0.10	37.1 ± 0.13
PH	7.42 ± 0.01	7.42 ± 0.01	7.39 ± 0.01
PO2, mm Hg	103 ± 4	107 ± 5	96 ± 4
PCO2, mm Hg	39 ± 1	40 ± 0	41 ± 1
plasma glucose, mg/dL	192 ± 11	215 ± 17	173 ± 12
hematocrit, %	44 ± 1	43 ± 1	43 ± 1
3h 15 min after recirculation			
rectal temperature (°C)	37.3 ± 0.19	36.7 ± 0.26	36.8 ± 0.19
cranial temperature (°C)	36.9 ± 0.44	37.0 ± 0.36	37.2 ± 0.20
1 day after treatment			
rectal temperature (°C)	37.3 ± 0.19	36.7 ± 0.26	36.8 ± 0.19
body weight (g)	289 ± 14	301 ± 12	294 ± 7
2 days after treatment			
rectal temperature (°C)	37.3 ± 0.14	37.4 ± 0.07	37.8 ± 0.25
body weight (g)	266 ± 14	293 ± 14	291 ± 8
3 days after treatment			
rectal temperature (°C)	36.7 ± 0.41	37.5 ± 0.26	37.8 ± 0.13
body weight (g)	227 ± 13	293 ± 16	287 ± 8 *
7 days after treatment			
rectal temperature (°C)	37.4 ± 0.39	37.3 ± 0.22	37.9 ± 0.26
body weight (g)	258 ± 18	320 ± 21	320 ± 12

values are mean ± SEM
MCAo, middle cerebral artery occlusion

* different from saline group ($p<0.01$, student's t-test).